UNIVERSITY of CALIFORNIA
SANTA CRUZ

AN ANALYSIS INTO THE AGN FRACTION IN DARK ENERGY SURVEY GALAXY CLUSTERS

A thesis submitted in partial satisfaction of the
requirements for the degree of

BACHELOR OF SCIENCE

in

PHYSICS

by

Raziq S. Noorali

7 December 2018

The thesis of Raziq S. Noorali is approved by:

Professor Tesla Jeltema
Advisor

Professor Robert P. Johnson
Chair, Department of Physics

Abstract

An Analysis into the AGN Fraction in Dark Energy Survey Galaxy Clusters

by

Raziq S. Noorali

The relationship between a galaxy's evolution and its supermassive black hole is not well understood and is an active topic of investigation. It is theorized that Active Galactic Nuclei (AGN) are part of a galaxy's life cycle and thus can be indicative of its phase of evolution. In this thesis, we use the Dark Energy Survey (DES) redMaPPer 6.4.22+2 catalog of galaxy clusters and Chandra archival data to investigate the correlation between the fraction of galaxies hosting AGN and cluster redshift and richness. We obtain a sample of 456 X-ray AGN in 26023 galaxies in 274 galaxy clusters using a Python matching program that crosschecks between both data sets. A preliminary analysis shows that, above a redshift of 0.4, there is a positive trend of AGN fraction and redshift and, below a redshift cut of 0.6, there is a negative trend of AGN and richness. Luminosity cuts are not made, so no large conclusions can be drawn.

Contents

Acknowledgements

I'd like to thank the following people for their amazing support throughout the process: Tesla Jeltema for being a fantastic mentor and for constantly believing in me; my eventual coauthor David Laubner for, without whom, this project would have never gotten off the ground; Devon Hollowood, for answering all of my technical questions; Spencer Everett for always taking the time to help me on science and on life, along with others in our research group at UC Santa Cruz.

1

Introduction

Galaxies and galaxy clusters provide a powerful probe of large-scale cosmology. By analyzing these connected objects, we can gain insight on a variety of concepts ranging from candidates for dark matter to potential dark energy evolution and insight into the large-scale structure of the universe [1]. Galactic evolution provides us a macroscopic view to gather information on the universe which can tighten the constraints on current cosmological models and give us a background to look for signatures of weakly interacting particles.

In this paper, we investigate the Active Galactic Nuclei (AGN) fraction of galaxy clusters compared to their richness and redshift in order to better understand the evolution of the galaxy compared to its supermassive black hole. We use data from the Chandra X-Ray Observatory and the redMaPPer catalogue through the Dark Energy Survey to provide these results.

The outline of the paper is as follows: Section 1 continues with an overview on galaxies, AGN, and various measurement parameters. Section 2 describes the methods, including a description of how the data sets are made and how we systematically select for

Active Galactic Nuclei (AGN) in galaxy clusters. Section 3 discusses the analysis of the data, including where we make cuts to our data and the calculation of the AGN fraction in various richness and redshift bins. Finally, section 4 contains a discussion on the analysis and the future work that this project will lead to.

1.1 Galaxies

Galaxies and galaxy clusters are some of the largest structures in the universe, with individual galaxies ranging from approximately 0.1 kilo-parsec(kpc) to 10 kpc in diameter, elliptical galaxies sometime exceeding this, and clusters with a diameter on the order of 2 mega-parsecs(Mpc)[2]. Galaxies typically contain large amounts of dark matter, which is a nonluminous form of matter that comprises as upwards of ninety percent of the mass of the galaxy[3]. Most galaxies have a supermassive black hole (SMBH) at their centers[1]. The relationship between the SMBH and the evolution of the galaxy on timescales equivalent to its lifetime is not well understood and is an active topic of investigation in astronomy.

1.2 AGN

When a SMBH accretes matter, the surrounding disk heats to high temperatures which emits bright electromagnetic radiation. Galaxies without this radiation at their core are classified as having a dormant nucleus [4], whereas galaxies with bright cores are classified as having AGN [1]. If a SMBH is actively accreting matter, the energy from this interaction will radiate all across the electromagnetic spectrum with energies up to the order of $10^{41} - 10^{46}$ ergs/sec, but this paper considers only X-ray emissions. When it no longer

accretes matter, it returns to its dormant state.

The SMBH can become active if there is new accretion of cold matter i.e. from a galaxy merger or active stellar evolution, and is linked to star formation in the galaxy [4]. Why AGN and stellar formation must be linked, however, is not well understood. AGN regulation and its subsequent feedback are also thought to affect the galaxy's ability to host star-forming regions, thus directly impacting its evolution, its host cluster and the intragalactic medium[5]. In addition, the mass of the center bulge of the galaxy is very strongly correlated to the mass of the SMBH[6]. Thus, we can consider this process to be indicative of the galaxys overall evolution and connect the previously disjoint relationship between the time evolution of the galaxy and the SMBH. In addition AGN are affected by the gas content accreting into the SMBH, and this can be affected by tidal forces [7] and galaxy mergers [8]. Since it is also known that galaxies in clusters evolve at different rates than galaxies in the field, this means that AGN can be affected by whether or not it exists in a cluster. We can compare intrinsic qualities of a cluster such as its redshift and richness to the fraction of AGN in the cluster [9].

1.2.1 Measurement Parameters

This section defines several terms used throughout this paper. Terms include redshift, galaxy member probability, richness, and AGN fraction.

Redshift is a measured parameter that describes how the wavelength of light emanating from a source is stretched, the systematic evaluation of which will be discussed in the Methods section. This can happen from the relativistic doppler shift of the object. Taking into account the velocity dispersion of the galaxy, we can surmise that this redshift

is caused by the cosmological expansion of space-time. From this redshift measurement, we can determine the luminosity distance of the object. By assuming a ΛCDM cosmological model of the universe[10], we reduce the Friedmann-Robertson-Walker metric[11] to get:

$$H(z) = H_0 \left(\Omega_m(1+z)^3 + \Omega_\gamma(1+z)^4 + \Omega_\Lambda\right) \tag{1.1}$$

where $H(z)$ is the Hubble Paremeter, Ω_M, Ω_γ[1], and Ω_Λ are dimensionless density parameters, H_0 is the Hubble Constant, and z is the redshift. From this, we can define the luminosity distance[12] as:

$$D_L = c(1+z)\int_0^z \frac{dz'}{H(z')} \tag{1.2}$$

Given known parameters from the Planck 2015 cosmological survey [13], we can determine this distance to find the luminosities of our objects using

$$L = 4\pi D_L^2 F \tag{1.3}$$

where F is the measured flux.

Since we observe astronomical data on the two dimensional sky, measured in Right Ascension (RA) and Declination (Dec), our coordinate for depth is redshift. Given uncertainty in redshift, there exists a possibility that the galaxy and the cluster associated with it may be unrelated. Thus we assign each galaxy a probability, called the **galaxy member probability**, that expresses how likely a given galaxy is to be part of a specific cluster. This probability is systematically determined by the redMaPPer algorithm, which will be discussed in Chapter 2.

When we consider the parameters of large scale cosmological objects, such as galaxy clusters, we want to be able to consider only direct observables. While it is possible

[1]The Astropy library in Python takes the limit as this term approaches zero

to infer parameters, such as the halo mass function for a certain number of galaxies [14], mass is not a direct observable and is very dependent on the the type of model that is used. Instead, we consider a mass-proxy called **richness** (λ), which is defined as the sum of the galaxy member probabilities of that cluster[15]. Using richness, we have an observable quantity that can be related to mass given the proper richness-mass function.

To understand AGN evolution, we use a metric called the **AGN fraction**, which is the fraction of galaxies with X-ray AGN. In a given redshift or richness bin, this is defined as[16]:

$$\text{AGN fraction} = \frac{\sum P_{\text{Mem AGN}}}{\sum P_{\text{Mem other}}} \tag{1.4}$$

where the numerator is the sum of the galaxy member probabilities of galaxies with AGN, $P_{\text{Mem AGN}}$, and the denominator is the sum of the galaxy member probabilities of all the galaxies in the appropriate bin, $P_{\text{Mem other}}$. We note that if we know exactly whether or not each galaxy belongs to a cluster, this fraction reduces to the total number of galaxies with AGN over the total number of galaxies in the appropriate bin. The error on the member probabilities is assumed to follow a Bernoulli distribution:

$$\sigma^2 = \sum_{i=1}^{N} p_i(1 - p_i) \tag{1.5}$$

where σ is the standard deviation, p_i is the probability of the galaxy in consideration, and the sum is over either all AGN host galaxies or all galaxies in the bin. This error is then propagated into the AGN fraction itself.

1.3 Data

We used two datasets for our study: The Dark Energy Survey(DES) and the Chandra Observatory data. These datasets are considered some of the most precise datasets for this purpose. We have access to the archival Chandra data, which is available to the public, and as DES members, we have access to the latest redMaPPer catalog.

1.3.1 Dark Energy Survey

The Dark Energy Survey is an international collaboration working to study large scale cosmological phenomena, such as the overall cosmological acceleration known as dark energy. Of the four different cosmological probes DES monitors, we will use primarily the set of galaxy clusters [17].

Using the Blanco 4 meter telescope at Cerro Tololo Inter-American Observatory (CTIO), DES spans nearly 5000 square degrees, including an overlap of stripe 82 of the Sloan Digital Sky Survey, covering the grizY photometric bands [17]. This survey contains approximately 310 million galaxies, some of which live in massive galaxy clusters identified by the red-sequence Matched-Filter Probabilistic Percolation (redMaPPer) Galaxy Cluster algorithm [18]. This dataset will be an order of magnitude larger than other studies (see [16]). The specific dataset used is the Year 3 redMaPPer catalog. We consider the version 6.4.22+2 full catalog with a richness cut of $\lambda > 20$.

1.3.2 Chandra

For X-ray source comparison, we use targeted and serendipitous imaging of DES clusters gathered by Chandra Advanced CCD Imaging Spectrometer (ACIS). The Chandra

X-ray Observatory (CXO), which is a component of NASAs Great Observatories, is devoted to the observation of photons with energies ranging from 0.08 keV(kilo-electron volt) to 10 keV. Its observations are further spread than the DES, so we only consider galaxies measured by both data sources such that their centers are within two arcseconds of each other [19, 20, 21]. We use the Chandra Interactive Analysis of Observations (CIAO) program to preform X-ray analysis into point source X-ray fluxes and place upper limits on X-ray undetected galaxies. This gives us a more refined way to discuss the AGN fraction.

1.4 Previous Research

Since the accretion of matter is one of the main drivers of AGN, we can surmise that this driver would be higher for small clusters and groups, where there is more chance for galaxy mergers which would contribute to the feeding of cold gas to the SMBH[8]. Previous studies have suggested that there is a strong positive correlation in redshift and the fraction of AGN in galaxy clusters (AGN fraction) which mirrors the fact that there is greater star formation in galaxies at higher redshift[22, 23]. However, a recent study on DES Verification Data has shown there is no correlation in cluster richness to AGN fraction [16]. This study, however, had a sample size that was too low to show mild trends. This motivates our study to further constrain these relations.

In this paper, we investigate the AGN fraction of galaxy clusters identified in the DES redMaPPer catalog and verified through Chandra archival data to better understand the relationship between an AGN and its environment. We consider the AGN fraction in redshift bins from $z = 0.2$ to $z = 1.0$ and richness bins from $\lambda = 20$ to $\lambda = 200$.

2

Methods

We use two external sources of analysis to facilitate our own: redMaPPer and CIAO. All other methods are done using scripts in Python version 3.7.1.

2.1 External Programs for Analysis

2.1.1 redMaPPer

The redMaPPer cluster finder algorithm is an optical cluster finder which looks for overdensities of galaxies starting with ones that fit the "red sequence" model, which is a typical set of elliptical or lenticular galaxies that have older stars and that are similar in redshift, giving them similar colors.

The algorithm first takes a set of galaxies with known redshifts and uses them to find overdensities of galaxies with a similar color nearby, thereby creating an empirical red sequence model. This algorithm then groups the galaxies in clusters based on color, connectivity, and distance from the center and assigns them a redshift based on the color

of the red sequence.

Since redMaPPer uses statistical methods to form clusters, each galaxy detected is assigned a certain probability of belonging to the cluster. The assigned richness is therefore the sum of the assigned member probabilities in the cluster. We will only consider clusters of $\lambda > 20$ which gives us 2,893,400 galaxies in 53,610 clusters. A detailed description of redMaPPer can be found in [18][24].

2.1.2 CIAO

CIAO is a program developed by the Chandra team as a general purpose interactive tool optimized for X-ray astronomy. CIAO focuses primarily on data manipulation and preparation, imaging, imaging and grating spectroscopy, timing analysis, and response tools. An in-depth description can be found at [25].

2.2 Cluster AGN Selection

2.2.1 Initial Galaxy and AGN Candidate Selection

We begin by considering where the Chandra field of view overlaps with the DES field of view. For each observation, we run a CIAO tool called *wavdetect*[1], which is a point source detection program that looks for excess flux given the shape of the off-axis point spread functions (PSF) at each position and returns point sources in the 0.3-7.9 keV range.

To obtain our AGN sample, we first cross-reference the positions of the DES redMaPPer galaxy member catalog and compare it to point sources determined by *wavdetect*. We consider points that are within two arcseconds of each other as determined by a

[1] http://cxc.harvard.edu/CIAO/ahelp/wavdetect.html

python script, which takes into account the respective errors of each instrument. To find matches, we first consider any intersecting points on a postage stamp in the sky, then find angular distances between X-ray and optical point sources.

Given the RA and Dec of two points, we can find the angular distance between them using the spherical law of cosines:

$$d = \arccos(\cos(90\,\mathrm{deg} - \delta_1)\cos(90\,\mathrm{deg} - \delta_2) + \sin(90\,\mathrm{deg} - \delta_1)\sin(90\,\mathrm{deg} - \delta_2)\cos(\alpha_1 - \alpha_2)) \tag{2.1}$$

where d is the angular distance between two points[2], α is the RA of the object and δ is the Dec. In our analysis, we use the AstroPy library's angular separation class[3], which uses Vincenty great circle formula to resolve beyond 32 bit floating point accuracy [26]. Afterwards we compile a catalog of galaxies belonging to clusters with at least one match from the above, noting which galaxies are considered AGN candidates.

With this catalog, we consider whether or not the centers of each galaxy are represented in at least one Chandra observation. To do this, we use CIAO's *find_chandra_obsid* tool[4] on each galaxy central point. From this, we note that there are sources in multiple Chandra observations, for which we only consider the observations with the longest exposure time.

2.2.2 Determining Luminosities

With sources across redshifts, we can consider that we are more likely to detect fainter sources that are closer to us. This presents an inherent bias in our analysis towards low redshift clusters. We can correct this by examining the luminosities of our AGN and

[2]This does not assume the small angle approximation
[3]http://docs.astropy.org/en/stable/coordinates/matchsep.html
[4]http://cxc.harvard.edu/CIAO/ahelp/find_chandra_obsid.html

only considering those that meet a certain threshold so that we are comparing similarly bright sources.

To find these luminosities, we use CIAO to obtain fluxes and its upper limits on each galaxy in order to make appropriate cuts on luminosity. To find the fluxes with CIAO, we use the *srcflux*[5] tool for each galaxy.

For *srcflux*, we must consider the emitted energy level range emitted by the source. As inputs, we find a lower bound, upper bound, and characteristic energy as given by:

$$E = \frac{E_i}{1+z} \tag{2.2}$$

where E is the emitted energy level, z is the redshift given by the redMaPPer catalog, and $E_i \in \{2.0, 3.8, 10\}$ keV, which outputs a typical a lower bound, characteristic energy, and upper bound respectively for X-ray AGN luminosity.

Throughout our Galaxy, there are clouds of neutral hydrogen that can absorb the flux from our AGN. It is important to consider how much is in line of sight, to account for errors in our detected flux. From radio surveys[27, 28], we can find the neutral hydrogen column density at a given RA and Dec and account for any flux that was absorbed.

To find the flux from *srcflux*, we input the neutral hydrogen column density, an ideal PSF input using a 95% confidence interval, the energy level range, and the specific Chandra observation ID to obtain fluxes.

After obtaining the fluxes and upper limits, we add flags to each of our entries, including whether it's an AGN candidate, an upper limit, and near a chip edge. Finally, using equation 1.3, we determine the luminosity of the object from the flux or upper limit if the former does not exist.

[5] http://cxc.harvard.edu/CIAO/ahelp/srcflux.html

3

Analysis

Through our cluster AGN selection, we obtain 26023 redMaPPer galaxies in 274 clusters, for which there are 456 AGN candidates. Looking at Figure 3.1, we can examine the distribution of redshifts and richnesses and determine appropriate bins for each. We will then consider the AGN fraction in these bins.

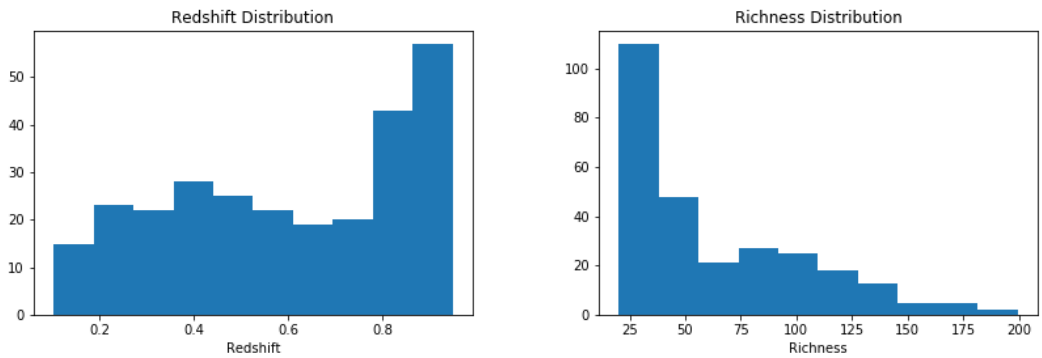

Figure 3.1: Distribution of redshifts (left) and richnesses (right) over the 274 identified redMaPPer clusters, distributed in 10 bins.

3.1 Luminosity Cuts

Determination of luminosities is currently ongoing. Because fluxes for the same luminosity decreases by the square of the distance, high redshift sources would be more difficult to detect, which means that we should expect to find only high luminosity sources at high redshift.

To take this trend into account, we will make an order of magnitude luminosity cut, which would effectively only consider high luminosity objects over all redshifts. Following from Bufanda et al, 2016, we would make a cut at 10^{43} ergs, however, the precise cut will be determined after luminosity calculations.

3.2 AGN Fraction in Redshift Bins

In this section, we present the AGN fraction in 15 redshift bins, the results of which are summarized in Table 3.2. This analysis does not contain any cuts on luminosity nor richness. We use redshift bins ranging from 0.067 to 1.0. We do not consider the bin 0.0 to 0.067 because it does not contain any samples.

From Table 3.1 and Figure 3.2, we can see a positive trend from $z = 0.4$ to $z = 1.0$, which is what we expect from previous findings [16, 22, 23, 29]. From $z = 0.1$ to $z = 0.4$, we see a downward trend that we would attribute to detecting more AGN at lower luminosities, and would expect that it would be accounted for in future analyses with a luminosity cut.

Redshift Bin	AGN Fraction	AGN	Non-AGN	σAGN Fraction
0.067-0.133	0.0309	18	499	0.0035
0.133-0.200	0.0167	16	804	0.0017
0.200-0.267	0.0140	29	1848	0.0010
0.267-0.333	0.0110	27	2123	0.0010
0.333-0.400	0.0099	24	2147	0.0009
0.400-0.467	0.0148	37	2396	0.0011
0.467-0.533	0.0081	23	1927	0.0011
0.533-0.600	0.0090	30	2604	0.0011
0.600-0.667	0.0172	38	1776	0.0019
0.667-0.733	0.0162	27	1459	0.0024
0.733-0.800	0.0105	27	1884	0.0017
0.800-0.867	0.0227	58	2305	0.0026
0.867-0.933	0.0246	89	3291	0.0025
0.933-1.000	0.0286	13	504	0.0059

Table 3.1: AGN fraction results. There is no luminosity cut on this data, but we only consider galaxy clusters with $\lambda > 20$. Column one shows the specific redshift bin. Column two shows the AGN fraction at that bin, calculated using Equation 1.4. Columns three and four have the number of galaxies with and without AGN and column five has the error on the AGN fraction out to one sigma. The membership probabilities have been accounted for in the calculation of the AGN fraction.

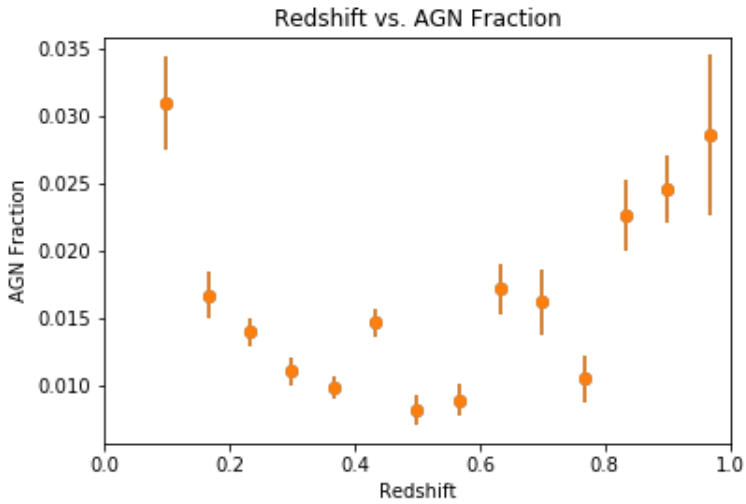

Figure 3.2: Evolution of the AGN fraction from $z = 0.1$ to $z = 1.0$ in bins described in Table 3.1 for clusters of $\lambda > 20$. There is no luminosity cut on this data. Points have been offset in the x direction for visual clarity.

3.3 AGN Fraction in Richness Bins

In this section, we present AGN fraction in 5 richness bins, the results of which are summarized in Table 3.2. This analysis does not contain any cuts on luminosity, however, a cut is made on redshift to account for biases with luminosity. We choose two cuts in redshift; $z < 0.6$ (low redshift) and $z > 0.6$ (high redshift) over richnesses from $20 < \lambda < 200$.

From Table 3.2 and Figure 3.3 we observe a negative trend at the $z < 0.6$ threshold and a weaker negative trend at $z > 0.6$ such that lower richness clusters have a higher AGN fraction. This agrees with our assumptions in Chapter 1 expecting more AGN in galaxies that have more mergers. While there is no luminosity cut and we would expect to detect more AGN at lower redshifts than at higher ones, it is not clear as to whether there is an inherent bias associated with this data. Additional work is needed to cut on luminosities and solidify this analysis.

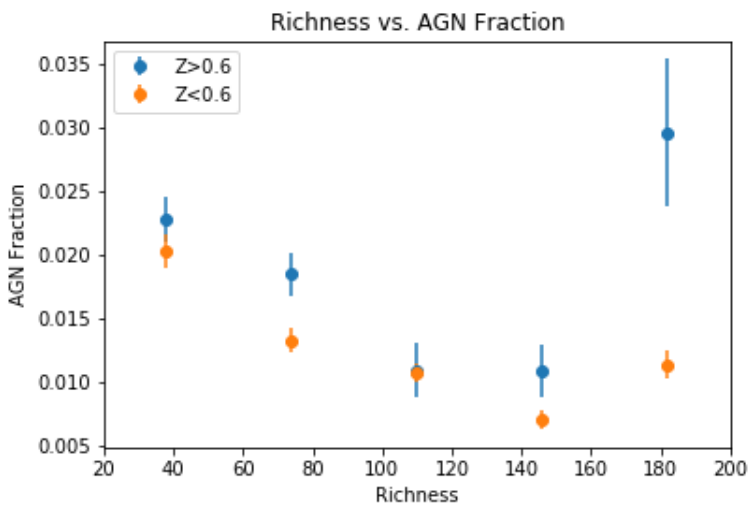

Figure 3.3: Evolution of the AGN fraction from $\lambda = 20$ to $\lambda = 200$ in bins described in Table 3.2 for clusters of $\lambda > 20$. There are two cuts at $z > 0.6$ and $z < 0.6$ and there are no luminosity cuts. Points have been offset in the x direction for visual clarity.

	Richness Bins	AGN Fraction	Number AGN	Number Other	σAGN Fraction
z<0.6	20-56	0.0203	65	2896	0.0013
	56-92	0.0133	38	2572	0.0010
	92-128	0.0108	62	5052	0.0007
	128-164	0.0071	29	2910	0.0007
	164-200	0.0114	10	918	0.0012
z>0.6	20-56	0.0228	143	5842	0.0018
	56-92	0.0185	62	2718	0.0017
	92-128	0.0110	19	1342	0.0022
	128-164	0.0109	13	944	0.0021
	164-200	0.0296	15	373	0.0058

Table 3.2: AGN fraction results. There is no luminosity cut on this data, but we only consider galaxy clusters with $\lambda > 20$. In addition, we consider cuts on redshift at $z > 0.6$ and $z < 0.6$. Column one shows the specific redshift bin. Column two shows the AGN fraction at that bin, calculated using Equation 1.4. Columns three and four have the number of galaxies with and without AGN and column five has the error on the AGN fraction out to one sigma. The membership probabilities have been accounted for in the calculation of the AGN fraction.

4

Future Work

The next step in our analysis is to conclude the luminosity measurements as described in Chapter 2. This way, we can apply proper cuts to our data and account for the selection bias that we have. This analysis is currently in progress and will fundamentally affect our trends, which prevents us from making any strong conclusions. However, this preliminary analysis points to a strong increase in AGN activity with redshift and for smaller clusters to have a higher AGN fraction.

This work can be further expanded. Additional datasets, such as the DES Y5 catalog, can be used to get a larger sample of AGN and can provide a deeper analysis. We can also consider clusters of richness $\lambda < 20$ in future analyses to better examine the effects on AGN in low richness clusters. To conserve computation time, we only considered a single Chandra observation per redMaPPer galaxy, thereby discounting when multiple X-ray observations were available at a single source. Including these observations would increase the statistical significance of our objects and improve the future analysis.

In future analyses, we can also consider some of the other features of the galaxy

on its AGN, such as its color and its distance from the core of its host's cluster. In addtion, we can consider field galaxies, which do not have a cluster associated with it. These environmental factors help to provide insight into the factors that can trigger of AGN.

Bibliography

[1] H. C. Ford, Z. I. Tsvetanov, L. Ferrarese, and W. Jaffe, (1997).

[2] S. Shen, H. J. Mo, S. D. M. White, M. R. Blanton, G. Kauffmann, W. Voges, J. Brinkmann, and I. Csabai, (2003).

[3] B.-A. Gradwohl and J. A. Frieman, The Astrophysical Journal **398**, 407 (1992).

[4] D. B. Sanders, B. T. Soifer, J. H. Elias, B. F. Madore, K. Matthews, G. Neugebauer, and N. Z. Scoville, The Astrophysical Journal **325**, 74 (1988).

[5] J. Silk and M. J. Rees, Astronomy and Astrophysics **331**, L1 (1998).

[6] D. J. Croton, V. Springel, S. D. M. White, G. De Lucia, C. S. Frenk, L. Gao, A. Jenkins, G. Kauffmann, J. F. Navarro, and N. Yoshida, Monthly Notices of the Royal Astronomical Society **365**, 11 (2006).

[7] R. Farouki and S. L. Shapiro, The Astrophysical Journal **243**, 32 (1981).

[8] D. O. Richstone, The Astrophysical Journal **204**, 642 (1976).

[9] Y.-Y. Choi, J.-H. Woo, and C. Park, (2009).

[10] A. Klypin, H. Zhao, and R. S. Somerville, The Astrophysical Journal **573**, 597 (2002).

[11] A. Mitra, Results in Physics **2**, 45 (2012).

[12] D. W. Hogg, arXiv:astro-ph/9905116 (1999), arXiv: astro-ph/9905116.

[13] P. Collaboration, P. a. R. Ade, N. Aghanim, M. Arnaud, M. Ashdown, J. Aumont, C. Baccigalupi, A. J. Banday, R. B. Barreiro, J. G. Bartlett, N. Bartolo, E. Battaner, R. Battye, K. Benabed, A. Benot, A. Benoit-Lvy, J.-P. Bernard, M. Bersanelli, P. Bielewicz, J. J. Bock, A. Bonaldi, L. Bonavera, J. R. Bond, J. Borrill, F. R. Bouchet, F. Boulanger, M. Bucher, C. Burigana, R. C. Butler, E. Calabrese, J.-F. Cardoso, A. Catalano, A. Challinor, A. Chamballu, R.-R. Chary, H. C. Chiang, J. Chluba, P. R. Christensen, S. Church, D. L. Clements, S. Colombi, L. P. L. Colombo, C. Combet, A. Coulais, B. P. Crill, A. Curto, F. Cuttaia, L. Danese, R. D. Davies, R. J. Davis, P. de Bernardis, A. de Rosa, G. de Zotti, J. Delabrouille, F.-X. Dsert, E. Di Valentino, C. Dickinson, J. M. Diego, K. Dolag, H. Dole, S. Donzelli, O. Dor, M. Douspis, A. Ducout, J. Dunkley, X. Dupac, G. Efstathiou, F. Elsner, T. A. Enlin, H. K. Eriksen, M. Farhang, J. Fergusson, F. Finelli, O. Forni, M. Frailis, A. A. Fraisse, E. Franceschi, A. Frejsel, S. Galeotta, S. Galli, K. Ganga, C. Gauthier, M. Gerbino, T. Ghosh, M. Giard, Y. Giraud-Hraud, E. Giusarma, E. Gjerlw, J. Gonzlez-Nuevo, K. M. Grski, S. Gratton, A. Gregorio, A. Gruppuso, J. E. Gudmundsson, J. Hamann, F. K. Hansen, D. Hanson, D. L. Harrison, G. Helou, S. Henrot-Versill, C. Hernndez-Monteagudo, D. Herranz, S. R. Hildebrandt, E. Hivon, M. Hobson, W. A. Holmes, A. Hornstrup, W. Hovest, Z. Huang, K. M. Huffenberger, G. Hurier, A. H. Jaffe, T. R. Jaffe, W. C. Jones, M. Juvela, E. Keihnen, R. Keskitalo, T. S. Kisner, R. Kneissl, J. Knoche, L. Knox, M. Kunz, H. Kurki-Suonio, G. Lagache, A. Lhteenmki, J.-M. Lamarre, A. Lasenby, M. Lattanzi, C. R. Lawrence, J. P. Leahy, R. Leonardi, J. Lesgourgues, F. Levrier, A. Lewis, M.

Liguori, P. B. Lilje, M. Linden-Vrnle, M. Lpez-Caniego, P. M. Lubin, J. F. Macas-Prez, G. Maggio, D. Maino, N. Mandolesi, A. Mangilli, A. Marchini, M. Maris, P. G. Martin, M. Martinelli, E. Martnez-Gonzlez, S. Masi, S. Matarrese, P. McGehee, P. R. Meinhold, A. Melchiorri, J.-B. Melin, L. Mendes, A. Mennella, M. Migliaccio, M. Millea, S. Mitra, M.-A. Miville-Deschnes, A. Moneti, L. Montier, G. Morgante, D. Mortlock, A. Moss, D. Munshi, J. A. Murphy, P. Naselsky, F. Nati, P. Natoli, C. B. Netterfield, H. U. Nrgaard-Nielsen, F. Noviello, D. Novikov, I. Novikov, C. A. Oxborrow, F. Paci, L. Pagano, F. Pajot, R. Paladini, D. Paoletti, B. Partridge, F. Pasian, G. Patanchon, T. J. Pearson, O. Perdereau, L. Perotto, F. Perrotta, V. Pettorino, F. Piacentini, M. Piat, E. Pierpaoli, D. Pietrobon, S. Plaszczynski, E. Pointecouteau, G. Polenta, L. Popa, G. W. Pratt, G. Przeau, S. Prunet, J.-L. Puget, J. P. Rachen, W. T. Reach, R. Rebolo, M. Reinecke, M. Remazeilles, C. Renault, A. Renzi, I. Ristorcelli, G. Rocha, C. Rosset, M. Rossetti, G. Roudier, B. Rouill d'Orfeuil, M. Rowan-Robinson, J. A. Rubio-Martn, B. Rusholme, N. Said, V. Salvatelli, L. Salvati, M. Sandri, D. Santos, M. Savelainen, G. Savini, D. Scott, M. D. Seiffert, P. Serra, E. P. S. Shellard, L. D. Spencer, M. Spinelli, V. Stolyarov, R. Stompor, R. Sudiwala, R. Sunyaev, D. Sutton, A.-S. Suur-Uski, J.-F. Sygnet, J. A. Tauber, L. Terenzi, L. Toffolatti, M. Tomasi, M. Tristram, T. Trombetti, M. Tucci, J. Tuovinen, M. Trler, G. Umana, L. Valenziano, J. Valiviita, F. Van Tent, P. Vielva, F. Villa, L. A. Wade, B. D. Wandelt, I. K. Wehus, M. White, S. D. M. White, A. Wilkinson, D. Yvon, A. Zacchei, and A. Zonca, Astronomy and Astrophysics **594**, A13 (2016).

[14] J. L. Tinker, A. V. Kravtsov, A. Klypin, K. Abazajian, M. S. Warren, G. Yepes, S. Gottlober, and D. E. Holz, The Astrophysical Journal **688**, 709 (2008), arXiv:

0803.2706.

[15] S. Andreon, Astronomy & Astrophysics **587**, A158 (2016).

[16] E. Bufanda, D. Hollowood, T. E. Jeltema, E. S. Rykoff, E. Rozo, P. Martini, T. M. C. Abbott, F. B. Abdalla, S. Allam, M. Banerji, A. Benoit-Lvy, E. Bertin, D. Brooks, A. Carnero Rosell, M. Carrasco Kind, J. Carretero, C. E. Cunha, L. N. da Costa, S. Desai, H. T. Diehl, J. P. Dietrich, A. E. Evrard, A. Fausti Neto, B. Flaugher, J. Frieman, D. W. Gerdes, D. A. Goldstein, D. Gruen, R. A. Gruendl, G. Gutierrez, K. Honscheid, D. J. James, K. Kuehn, N. Kuropatkin, M. Lima, M. a. G. Maia, J. L. Marshall, P. Melchior, R. Miquel, J. J. Mohr, R. Ogando, A. A. Plazas, A. K. Romer, P. Rooney, E. Sanchez, B. Santiago, V. Scarpine, I. Sevilla-Noarbe, R. C. Smith, M. Soares-Santos, F. Sobreira, E. Suchyta, G. Tarle, D. Thomas, D. L. Tucker, A. R. Walker, and D. E. S. Collaboration, Monthly Notices of the Royal Astronomical Society **465**, 2531 (2017).

[17] A. Drlica-Wagner, I. Sevilla-Noarbe, E. S. Rykoff, R. A. Gruendl, B. Yanny, D. L. Tucker, B. Hoyle, A. Carnero Rosell, G. M. Bernstein, K. Bechtol, M. R. Becker, A. Benoit-Lvy, E. Bertin, M. Carrasco Kind, C. Davis, J. de Vicente, H. T. Diehl, D. Gruen, W. G. Hartley, B. Leistedt, T. S. Li, J. L. Marshall, E. Neilsen, M. M. Rau, E. Sheldon, J. Smith, M. A. Troxel, S. Wyatt, Y. Zhang, T. M. C. Abbott, F. B. Abdalla, S. Allam, M. Banerji, D. Brooks, E. Buckley-Geer, D. L. Burke, D. Capozzi, J. Carretero, C. E. Cunha, C. B. D'Andrea, L. N. da Costa, D. L. DePoy, S. Desai, J. P. Dietrich, P. Doel, A. E. Evrard, A. Fausti Neto, B. Flaugher, P. Fosalba, J. Frieman, J. Garca-Bellido, D. W. Gerdes, T. Giannantonio, J. Gschwend, G. Gutierrez, K. Honscheid, D. J. James, T. Jeltema, K. Kuehn, S. Kuhlmann, N. Kuropatkin, O.

Lahav, M. Lima, H. Lin, M. a. G. Maia, P. Martini, R. G. McMahon, P. Melchior, F. Menanteau, R. Miquel, R. C. Nichol, R. L. C. Ogando, A. A. Plazas, A. K. Romer, A. Roodman, E. Sanchez, V. Scarpine, R. Schindler, M. Schubnell, M. Smith, R. C. Smith, M. Soares-Santos, F. Sobreira, E. Suchyta, G. Tarle, V. Vikram, A. R. Walker, R. H. Wechsler, J. Zuntz, and D. E. S. Collaboration, The Astrophysical Journal Supplement Series **235**, 33 (2018).

[18] E. S. Rykoff, E. Rozo, D. Hollowood, A. Bermeo-Hernandez, T. Jeltema, J. Mayers, A. K. Romer, P. Rooney, A. Saro, C. Vergara Cervantes, R. H. Wechsler, H. Wilcox, T. M. C. Abbott, F. B. Abdalla, S. Allam, J. Annis, A. Benoit-Lvy, G. M. Bernstein, E. Bertin, D. Brooks, D. L. Burke, D. Capozzi, A. Carnero Rosell, M. Carrasco Kind, F. J. Castander, M. Childress, C. A. Collins, C. E. Cunha, C. B. D'Andrea, L. N. da Costa, T. M. Davis, S. Desai, H. T. Diehl, J. P. Dietrich, P. Doel, A. E. Evrard, D. A. Finley, B. Flaugher, P. Fosalba, J. Frieman, K. Glazebrook, D. A. Goldstein, D. Gruen, R. A. Gruendl, G. Gutierrez, M. Hilton, K. Honscheid, B. Hoyle, D. J. James, S. T. Kay, K. Kuehn, N. Kuropatkin, O. Lahav, G. F. Lewis, C. Lidman, M. Lima, M. a. G. Maia, R. G. Mann, J. L. Marshall, P. Martini, P. Melchior, C. J. Miller, R. Miquel, J. J. Mohr, R. C. Nichol, B. Nord, R. Ogando, A. A. Plazas, K. Reil, M. Sahln, E. Sanchez, B. Santiago, V. Scarpine, M. Schubnell, I. Sevilla-Noarbe, R. C. Smith, M. Soares-Santos, F. Sobreira, J. P. Stott, E. Suchyta, M. E. C. Swanson, G. Tarle, D. Thomas, D. Tucker, S. Uddin, P. T. P. Viana, V. Vikram, A. R. Walker, Y. Zhang, and D. E. S. Collaboration, The Astrophysical Journal Supplement Series **224**, 1 (2016).

[19] G. O. Abell, Annual Review of Astronomy and Astrophysics **3**, 1 (1965).

[20] T. Jeltema, Chandra Proposal 5081 (2017).

[21] M. C. Weisskopf, B. Brinkman, C. Canizares, G. Garmire, S. Murray, and L. P. V. Speybroeck, Publications of the Astronomical Society of the Pacific **114**, 1 (2002).

[22] P. Martini, E. D. Miller, M. Brodwin, S. A. Stanford, A. H. Gonzalez, M. Bautz, R. C. Hickox, D. Stern, P. R. Eisenhardt, A. Galametz, D. Norman, B. T. Jannuzi, A. Dey, S. Murray, C. Jones, and M. J. I. Brown, The Astrophysical Journal **768**, 1 (2013).

[23] P. Martini, G. R. Sivakoff, and J. S. Mulchaey, The Astrophysical Journal **701**, 66 (2009).

[24] E. S. Rykoff, E. Rozo, M. T. Busha, C. E. Cunha, A. Finoguenov, A. Evrard, J. Hao, B. P. Koester, A. Leauthaud, B. Nord, M. Pierre, R. Reddick, T. Sadibekova, E. S. Sheldon, and R. H. Wechsler, The Astrophysical Journal **785**, 104 (2014), arXiv: 1303.3562.

[25] A. Fruscione, J. C. McDowell, G. E. Allen, N. S. Brickhouse, D. J. Burke, J. E. Davis, N. Durham, M. Elvis, E. C. Galle, D. E. Harris, D. P. Huenemoerder, J. C. Houck, B. Ishibashi, M. Karovska, F. Nicastro, M. S. Noble, M. A. Nowak, F. A. Primini, A. Siemiginowska, R. K. Smith, and M. Wise, Society of Photo-Optical Instrumentation Engineers (SPIE) Conference Series **6270**, 62701V (2006).

[26] T. Vincenty, Survey Review **23**, 88 (1975).

[27] P. M. W. Kalberla, W. B. Burton, D. Hartmann, E. M. Arnal, E. Bajaja, R. Morras, and W. G. L. Pppel, Astronomy and Astrophysics **440**, 775 (2005).

[28] J. M. Dickey and F. J. Lockman, Annual Review of Astronomy and Astrophysics **28**, 215 (1990).

[29] J. Eastman, P. Martini, G. Sivakoff, D. D. Kelson, J. S. Mulchaey, and K.-V. Tran, The Astrophysical Journal Letters **664**, L9 (2007).